Hindawi
International Journal of Antennas and Propagation
Volume 2022, Article ID 9466510, 16 pages
https://doi.org/10.1155/2022/9466510

Research Article

Experimental Study on Dynamic Aerodynamic Characteristics of Different Antenna Aspect Ratios with Reduced Frequency

Yanqi Zhang and Zhaoming Zhang

Key Lab of Ministry of Industry and Information Technology for Unsteady Aerodynamics and Flow Control, College of Aerospace Engineering, Nanjing University of Aeronautics and Astronautics, Nanjing, Jiangsu 210016, China

Correspondence should be addressed to Yanqi Zhang; yanqizhang_nuaa@163.com

Received 2 December 2021; Revised 2 March 2022; Accepted 19 April 2022; Published 13 May 2022

Academic Editor: Raffaele Solimene

Radar antennas in the open air are affected by dynamic wind loading during azimuthal scanning. In this state, the acquisition and prediction of the aerodynamic load is the focus of the structure design for the antenna. We performed wind tunnel force tests on flat plate antennas with different aspect ratios. The changes in mean, maximum, and root mean square values of the aerodynamic coefficients relative to the antenna aspect ratio and reduced frequency are given for the first time. The effects of the antenna aspect ratio and reduced frequency on aerodynamic characteristics are analyzed. The experimental results indicate that the magnitude of the azimuthal moment is related to the antenna aspect ratio and the reduced frequency. It is worth noting that the antenna aspect ratio has a significant impact on the mean, maximum, and root mean square values of dynamic aerodynamic coefficients. The mean, maximum, and root mean square values of the rolling moment coefficient, azimuth moment coefficient, and pitching moment coefficient monotonously decrease with the increase in aspect ratio. In addition, the influence of reduced frequency on the dynamic aerodynamic coefficient is closely related to the antenna aspect ratio. Under the same antenna aspect ratio, increasing the reduced frequency will increase the mean, maximum, and root mean square values of the aerodynamic coefficient. For flat plate antennas with different aspect ratios, at the condition of increasing the aspect ratios, the mean, maximum, and root mean square values of aerodynamic coefficients do not change significantly with the change of reduced frequency.

1. Introduction

With the diversification and rapid development of antenna applications, the demand for radar antennas is increasing day by day [1–3]. Large flat plate antennas in open areas are easily affected by strong winds, such that the pitching moment of the antenna to the ground can exceed 100 tons·m [4]. In addition, antennas are required to rotate stably and with high precision; thus, wind loading is a key factor that must be considered in designing the radar antenna structure and developing the servo system [5–7]. Unlike stationary antennas, radar antennas that rotate azimuthally during operation are subjected to varying dynamic wind loads over time, which causes serious fatigue. Therefore, when designing this kind of antenna, designers should consider the aerodynamic characteristics of the antenna to ensure the safe and reliable operation of the radar [8]. Aerodynamic coefficients and the surface pressure coefficient are important parameters in designing for wind resistance design and verifying the structural strength of radar antennas [9]. Because of the difficulty of measuring wind loading in the field, researchers measure wind loading on antennas using wind tunnel tests to explore the aerodynamic characteristics of antennas. To ensure that the results of wind tunnel force tests can be used in the actual design of a radar antenna, Gawronski et al. [10] measured wind loading on the antenna on-site and verified the feasibility and accuracy of obtaining the aerodynamic coefficient of the antenna using wind tunnel test. In addition, Gumusel et al. [11] proved the feasibility of using numerical simulation of the flow field around an antenna to obtain the aerodynamic characteristics of the antenna, so as

to achieve the goal of optimizing the aerodynamic shape of antenna. It is worth noting that there have been a lot of experimental studies on the static aerodynamic characteristics of the antenna [5, 12, 13], but there is a lack of research on the aerodynamic characteristics of antenna azimuth rotation.

In the early stages of the study on aerodynamic characteristics of antennas during azimuthal rotation, Sachs [14] assumed that the pressure coefficient is uniformly distributed in the upper and lower half planes of the flat plate antenna along the span direction. Sachs gave the concept of reduced frequency, derived the semiempirical formula, and used the formula to convert the drag and azimuthal moment when the antenna is stationary into the dynamic azimuthal moment when the antenna is rotating. In recent years, with the diversification of means, obtaining aerodynamic characteristics of antennas using wind tunnel tests and numerical simulation has become a research hotspot [11, 15–17]. Lombardi [18] used wind tunnel force tests to study aerodynamic force on a rotating antenna. The study proved that the aerodynamic force coefficient when an antenna is rotating is different from the aerodynamic force coefficient when the antenna is stationary and proposed the limitation of obtaining the azimuthal moment result using the semiempirical formula [14]. Camci and Gumusel [17] and Gumusel et al. [11] studied the interaction between wake and the antenna body during antenna rotation based on the numerical simulation results of the flow field. They proved the feasibility of using numerical simulation to obtain the aerodynamic characteristics of an antenna. Although many numerical simulation studies on the aerodynamic characteristics of existing antennas [11, 19, 20], simulation results for aerodynamic characteristics during antenna rotation still lack the support of wind tunnel tests, and most studies only focus on aerodynamic characteristics when an antenna is stationary. Insufficiency of the research on aerodynamic characteristics during antenna rotation has become a limiting factor in the improvement and optimization of the antenna structure. Although wind tunnel tests are the most important and reliable means of obtaining the aerodynamic characteristics of antennas, because of limitations on test conditions and cycles, it is impossible to subject each antenna to such tests. Therefore, designers must understand the aerodynamic characteristics of typical antenna structures to facilitate the estimation of aerodynamic loads of antennas in the future [21].

Using a dynamic force test platform of a radar antenna wind tunnel, we perform force tests on antennas under different aspect ratios and reduced frequencies. The influence of the aspect ratio on aerodynamic characteristics of the antenna during azimuthal rotation and the change in aerodynamic coefficients compared to the reduced frequency is given. Our results provide a reference for stiffness and strength checks for flat plate antennas, help experts select an appropriate driving motor and related design, are conducive to estimating the aerodynamic load of a flat plate antenna, and aid designers in evaluating more comprehensively and accurately the impact of wind loading on antenna design.

2. Materials and Methods

2.1. Test Model. The experiment was carried out in an NH-2 wind tunnel at Nanjing University of Aeronautics and Astronautics. The dimension of the test section is 3 m (width) × 2.5 m (height) × 6 m (length). The contraction ratio of the wind tunnel is 2.89:1; the velocity range is 0–93 m/s; and the turbulence intensity range is 0.10–0.14%. The radar antenna model is divided into three main parts: the antenna array, the elevation angle adjustment mechanism, and a support rod, as shown in Figures 1(a) and 1(b). The antenna array is made of acrylic, and the other parts are made of steel. Wind tunnel dynamic force tests are performed on four flat plate antennas with aspect ratios AR = 0.5, 1.5, 2.0, and 2.5. When the antenna aspect ratio is less than 1, the rotation radius of the antenna is less than the height of the antenna. Except for the dimensions of the antenna array, the dimensions of the other parts of the model are the same. This paper mainly focuses on differences in the aerodynamic characteristics of antennas with different aspect ratios in their reduced frequency range. Table 1 gives the antenna model sizes and test conditions in their respective working ranges, in which the reduced frequency K is a dimensionless parameter, $K = (N \times D)/V$, where N is the rotational angular velocity, V is the incoming wind speed, and D is the antenna rotation diameter [14]. Because the support rod is part of the radar antenna and the blocking rate is less than 2.5% [5], support interference and blockage correction are not required for the test results.

2.2. Test Device. The radar antenna dynamic force measurement test platform can drive the azimuthal rotation of the model and real-time acquisition of aerodynamic force. The platform is composed of a motion control system and data acquisition system, as shown in Figure 2(a). The lower end of the model support rod is connected to the strain balance, and both are installed on the torque motor; the upper end of the rod is connected to the elevation angle adjustment mechanism with a fixed pin, as shown in Figure 2(b). The antenna elevation angle can be adjusted at an interval of 10° within the range of $\alpha = 0^\circ \sim 30^\circ$ by adjusting mechanism. The motion control mechanism is composed of a torque motor, encoder, optoelectronic, servo driver, motion control card, computer, and other parts. As shown in Figure 2(c), the rotation frequency range of the model is 0–4 Hz. During the test, the computer with a motion control card controls the output voltage of the servo driver to adjust the speed of the torque motor. The strain balance is connected to a low-pass filter amplifier with a slip ring, and the voltage signal output by the balance is collected by a computer equipped with a data acquisition card.

2.3. Test Data Processing. In the wind tunnel dynamic force test, the influence of gravity and inertia on the test results needs to be excluded. When the wind tunnel is not blowing, the electrical signal output by the balance when the antenna model rotates is collected as the initial reading and subtracted from the following blowing data. Finally, the

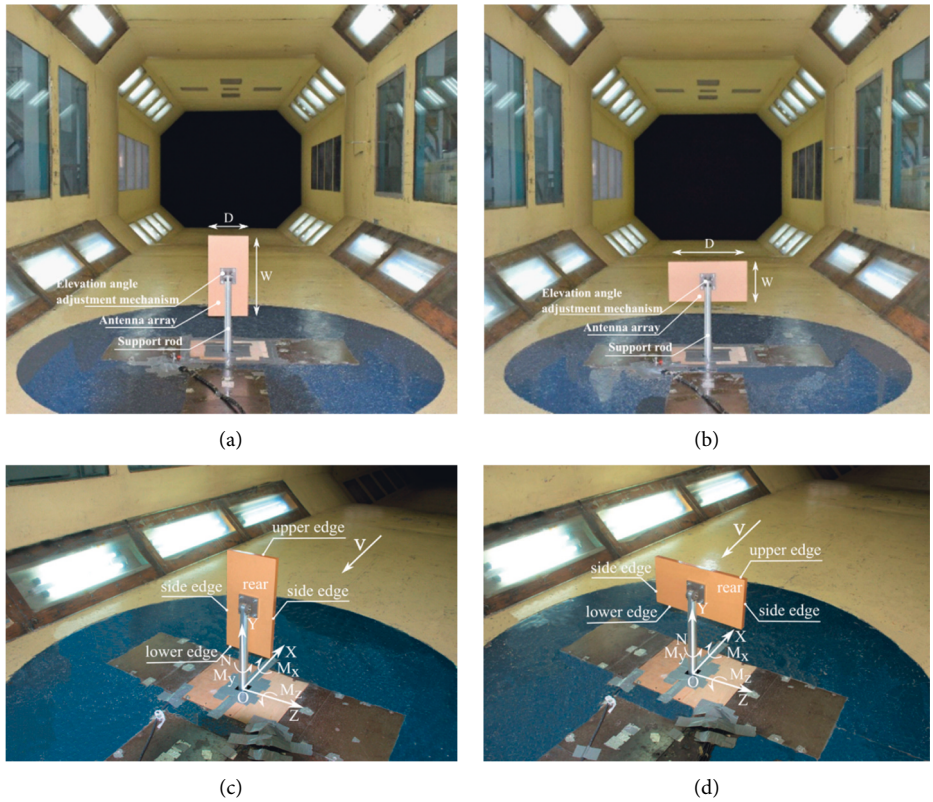

Figure 1: Definition of each part of radar antenna model and balance coordinate system. (a) AR<1. (b) AR≥1. (c) AR<1. (d) AR≥1. AR, aspect ratio.

Table 1: Dimensions of the antenna model and test conditions.

Aspect ratio (AR = D/W)	Length (D) × width (W) × thickness (C) (mm)	Elevation angle, α (°)	Blocking rate, δ (%)	Wind speed (m/s)	Reduced frequency, K
0.5	200 × 400 × 20	0	<1.5	16	0.06/0.09/0.12/0.15/0.2
1.5	300 × 200 × 20	0	<1.5	22	0.07/0.1/0.12/0.17/0.2
2.0	400 × 200 × 20	0	<1.5	18	0.12/0.2/0.25/0.31/0.37
2.5	500 × 200 × 20	0	<1.5	15	0.12/0.2/0.27/0.34/0.4

electrical signal is converted into aerodynamic coefficient data through the balance formula and wind axis-body axis formula. The six aerodynamic coefficients are given in the wind axis coordinate system as follows: drag coefficient $C_x = F_x/(0.5 \times \rho \times V^2 \times S)$, lift coefficient $C_y = F_y/(0.5 \times \rho \times V^2 \times S)$, lateral force coefficient $C_z = F_z/(0.5 \times \rho \times V^2 \times S)$, rolling moment coefficient $C_{mx} = M_x/(0.5 \times \rho \times V^2 \times S \times L)$, azimuthal moment coefficient $C_{my} = M_y/(0.5 \times \rho \times V^2 \times S \times L)$, and pitching moment coefficient $C_{mz} = M_z/(0.5 \times \rho \times V^2 \times S \times L)$, where ρ is the air density (kg/m^3), V is the wind velocity (m/s), reference area $S = D \times W$ (m^2), and reference length $L = D$ (m), as shown in Figures 1(c) and 1(d). Because the antenna rotates periodically and the lift coefficient C_y has little effect on the design of the radar antenna structure [22], we only discuss the drag coefficient C_x, the lateral force coefficient C_z, the rolling moment coefficient C_{mx}, the azimuthal moment coefficient C_{my}, and the pitching moment coefficient C_{mz} of the antenna in a single rotation period. Figure 3 shows the raw output signal of the balance after subtracting the initial reading and the signal filtered by the filtering method in Gustafsson [23]. The figure shows that the filtered signal follows the raw signal well. Zhang and Zhang [24, 25] introduce the test platform used in this paper and data processing methods.

2.4. Simulation Method. The numerical simulation results of the flow field can provide more abundant flow field information than wind tunnel tests. According to the method used in reference [25], the numerical simulation results of

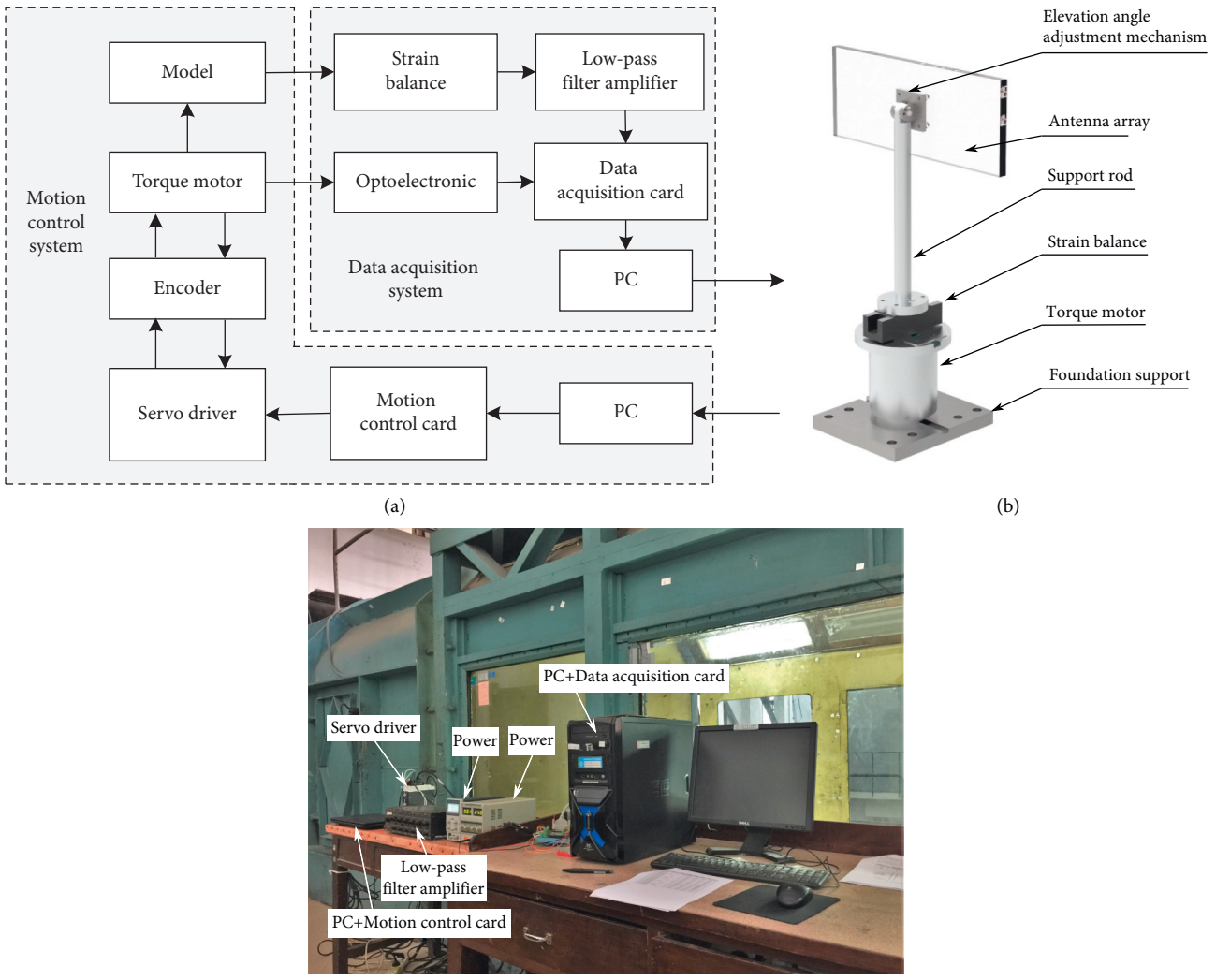

Figure 2: Connection diagram of test device and equipment: (a) schematic diagram of the motion control system and data acquisition system, (b) motion control system, and (c) data acquisition system.

antennas with different aspect ratios under corresponding wind tunnel test conditions are obtained in this paper. In order to test the accuracy of numerical simulation results, taking the flat plate radar antenna with aspect ratio AR = 2.0, $K = 0.12$, and $V = 15$ m/s as an example, the wind tunnel test results of the dynamic aerodynamic coefficient are compared with the numerical simulation results, as shown in Figure 4. It can be seen from the figure that in a rotation cycle, the numerical simulation results are in good agreement with the wind tunnel test results, meeting the requirements of comparative research [26].

3. Results and Discussion

An aerodynamic shape and structural optimization are essential parts of antenna design. The aerodynamic characteristics of antennas with different aspect ratios at the same wind speed differ significantly, which has attracted researchers' attention [14]. The effects of the aspect ratio and reduced frequency on the aerodynamic characteristics of antennas during azimuthal rotation are discussed below.

3.1. Aerodynamic Coefficients with Respect to the Aspect Ratio When $K = 0.12$. Figure 5 shows the change in the aerodynamic coefficients of the antenna with respect to the aspect ratio when the reduced frequency $K = 0.12$. The peak value of C_x enhances with the increasing aspect ratio, which is the same as the force test results of Ortiz et al. [27] for a stationary antenna. In addition, increasing the antenna aspect ratio reduces the positive peak value of C_{mz}, resulting in a decrease in the peak-to-peak value of C_{mz}. Changing the antenna aspect ratio significantly impacts the azimuthal position corresponding to the peak value of the aerodynamic coefficient. The C_x peak appears in advance with an increase in the aspect ratio, whereas the peak C_z, C_{mx}, C_{my}, and C_{mz} lag with an increase in the aspect ratio. It is worth noting that

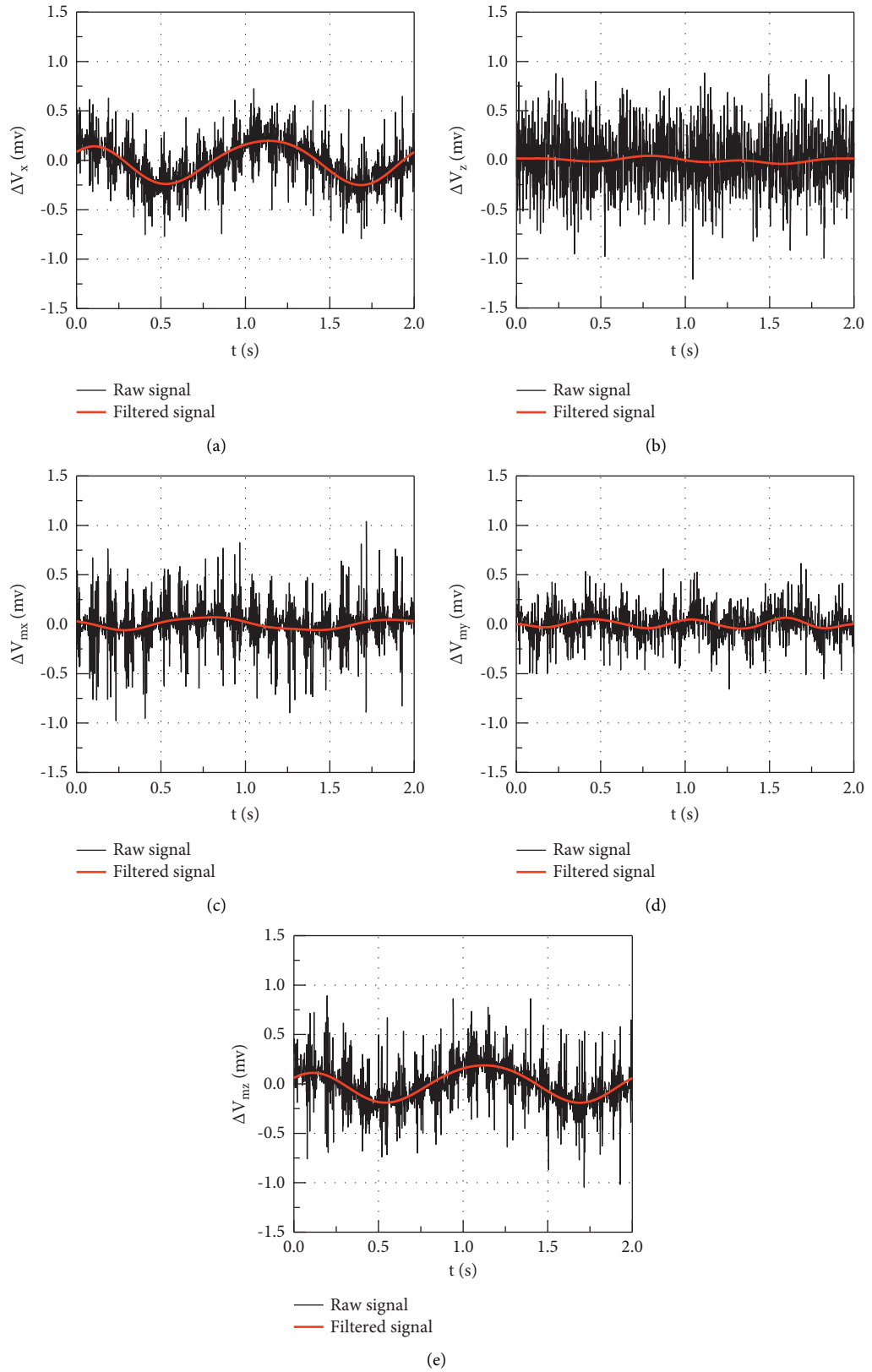

Figure 3: Raw and filtered signal output by the strain balance with respect to the acquisition time. The zero-point reference set has been subtracted (a) $\Delta V_x - t$, (b) $\Delta V_z - t$, (c) $\Delta V_{mx} - t$, (d) $\Delta V_{my} - t$, and (e) $\Delta V_{mz} - t$ ($K = 0.12$, $\alpha = 0^\circ$, and $t = 2$ s).

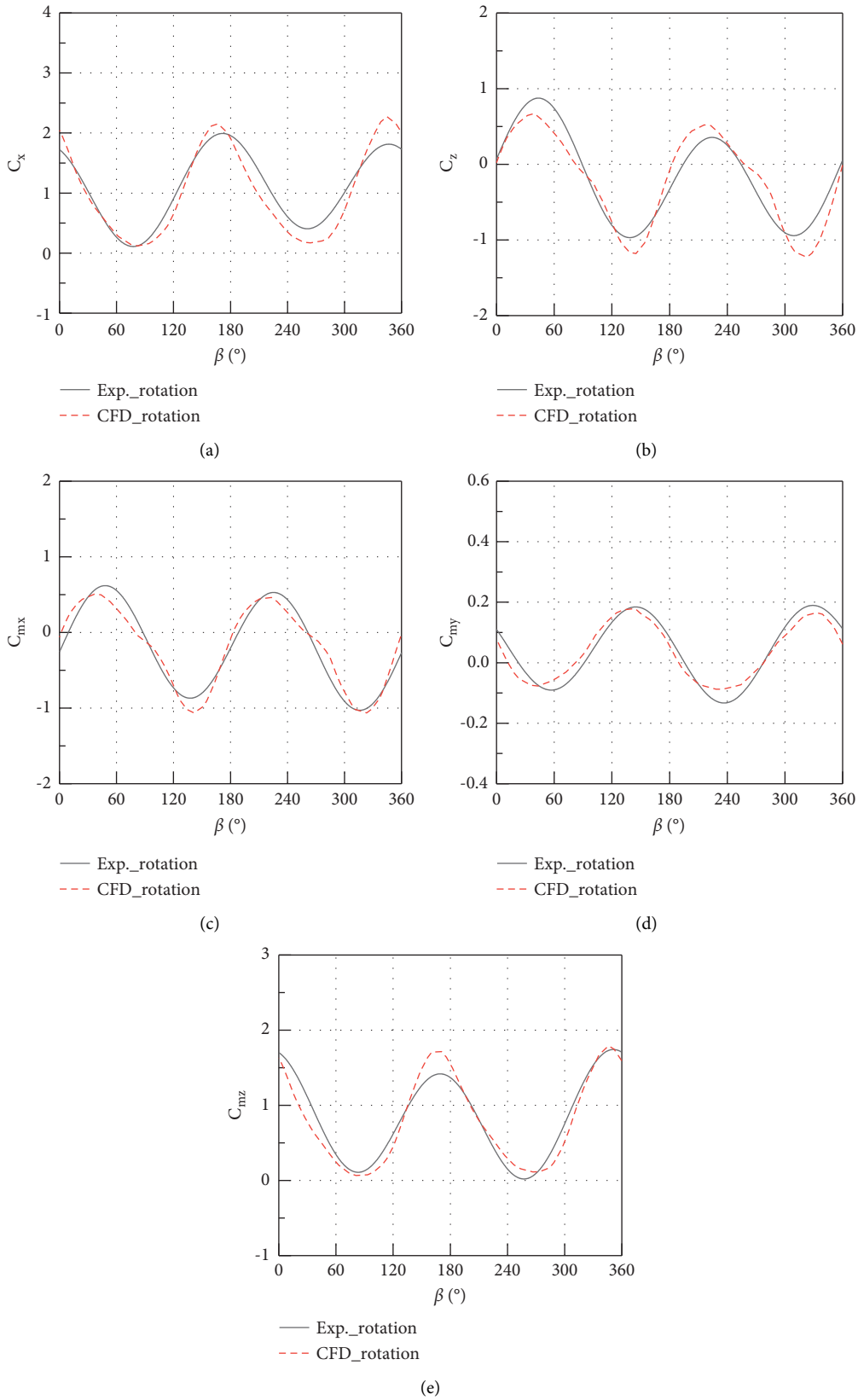

Figure 4: Comparison between test results and simulation results of antenna dynamic aerodynamic coefficient: (a) $C_x - \beta$, (b) $C_z - \beta$, (c) $C_{mx} - \beta$, (d) $C_{my} - \beta$, and (e) $C_{mz} - \beta$.

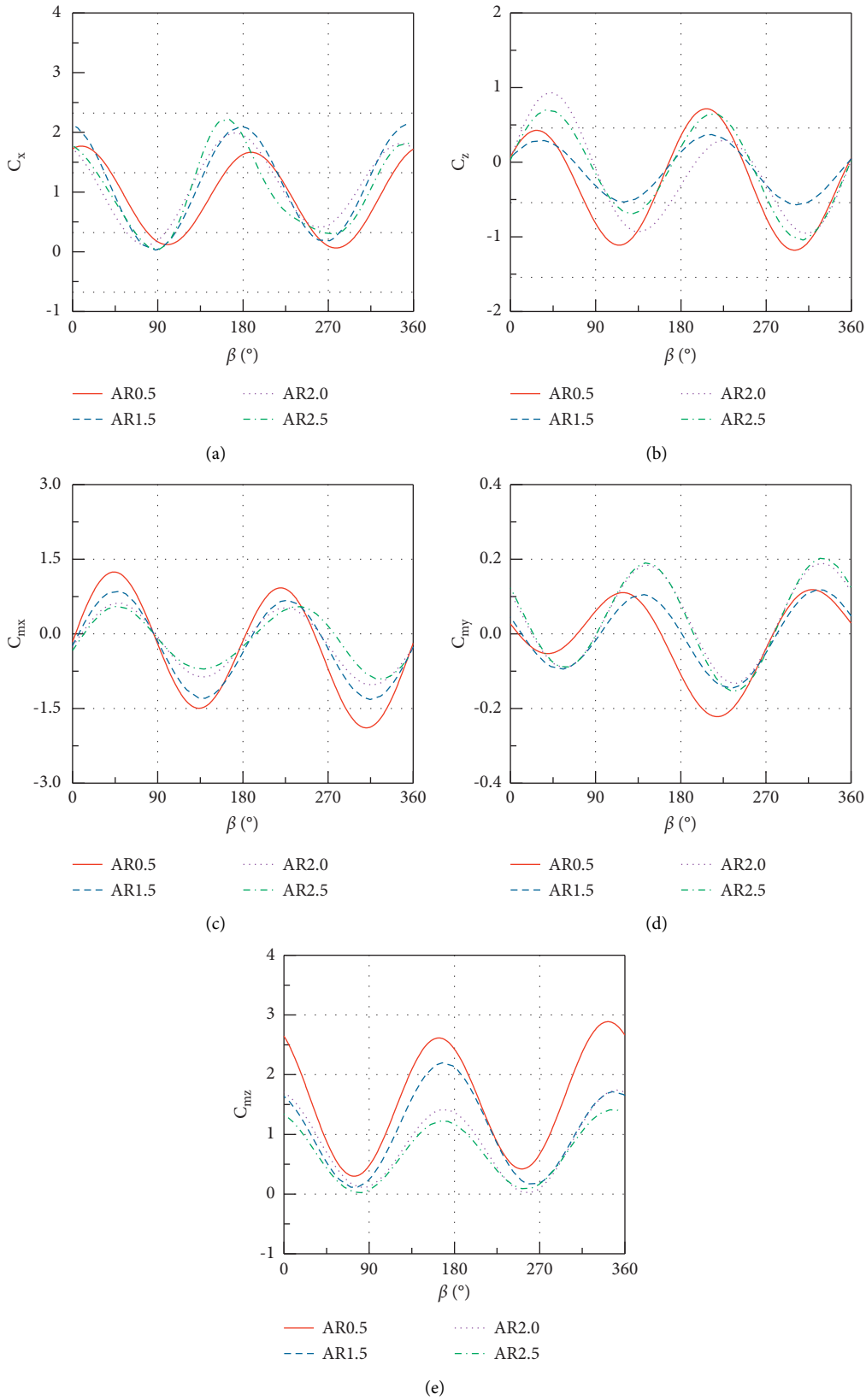

Figure 5: Aerodynamic coefficients with respect to the aspect ratio ($K = 0.12$): (a) $C_x - \beta$, (b) $C_z - \beta$, (c) $C_{mx} - \beta$, (d) $C_{my} - \beta$, and (e) $C_{mz} - \beta$.

when the antenna aspect ratio increases from 0.5 to 2.5, the lag of the corresponding azimuthal angle when the peak C_{my} appears exceeds 15°. The reason for this phenomenon is the difference between the two flow fields. This phenomenon is explained by analyzing Zhang and Zhang's research [25].

In a single rotation period, the smaller the peak-to-peak value of the aerodynamic coefficient, the smaller the change in dynamic wind loading on the antenna, which ensures that when the radar antenna is rotating azimuthally, the servo system is able to keep the antenna running smoothly. When $0.5 \le \mathrm{AR} < 2$, the aerodynamic coefficients in each direction change with the azimuthal angle and are more sensitive to a change in the aspect ratio. As the aspect ratio increases from 0.5 to 1.5, the change in peak-to-peak values of C_x, C_{my}, and C_{mz} is 24.1%, −74.8%, and −19.2%, respectively, and the maximum change is 21.2%, −34.4%, and −23.8%, respectively, where a positive value represents an increase and a negative value represents a decrease. Increasing the aspect ratio can significantly reduce the peak-to-peak and maximum values of the azimuthal moment coefficient and the pitching moment coefficient; when $2.0 \le \mathrm{AR} \le 2.5$, the variation of the aerodynamic coefficient with azimuth is not sensitive to the change in the aspect ratio. As the aspect ratio increases from 2.0 to 2.5, the change in peak-to-peak values of C_x, C_{my}, and C_{mz} is 16.5%, 10.9%, and −19.0%, respectively, and the maximum change is 12.1%, 7.4%, and −18.8%, respectively. At this point, increasing the aspect ratio can significantly reduce the pitching moment coefficient. In summary, the antenna aspect ratio increases from 0.5 to 2.5 for the peak-to-peak and maximum values of the aerodynamic coefficients, the drag coefficient always increases, the azimuthal moment coefficient first decreases and then increases, and the pitching moment coefficient always decreases. The peak-to-peak values of the aerodynamic coefficients can be used to determine the height of the antenna's windproof leg, and the maximum and root mean square values of the aerodynamic coefficients can be used for other calculations as appropriate.

3.2. Aerodynamic Coefficients with Respect to the Aspect Ratio When $K = 0.2$. Figure 6 shows the change in the aerodynamic coefficients of the antenna with respect to the aspect ratio when the reduced frequency $K = 0.2$. As shown in Figure 5, compared to $K = 0.12$, increasing the reduction frequency not only makes the overall aerodynamic coefficient larger but also increases the sensitivity of the aerodynamic coefficient to the antenna aspect ratio. Compared to the $\mathrm{AR} \ge 1$, when $\mathrm{AR} < 0.5$, C_{mx}, C_{my}, and C_{mz} vary significantly with the azimuthal angle. Therefore, when designing a flat plate antenna, it is necessary to obtain the aerodynamic coefficients at different working reduced frequencies, especially at the maximum reduced frequency. When $\mathrm{AR} < 2.0$, the aspect ratio significantly influences the aerodynamic coefficients in each direction compared to the azimuthal angle. When $\mathrm{AR} < 1.0$, the peak value of the aerodynamic moment changes significantly in all directions. As the aspect ratio increases from 0.5 to 1.5, the change in peak-to-peak values of C_x, C_{my}, and C_{mz} is −3.3%, −18.9%, and −22.6%, respectively, and the maximum change is 5.6%, −39.7%, and −29.6%, respectively. In addition, as the aspect ratio increases, the peak-to-peak and maximum values of the drag coefficient change little, whereas the peak-to-peak and maximum values of the azimuthal moment coefficient and the pitching moment coefficient change significantly. When $2.0 \le \mathrm{AR} \le 2.5$, the aspect ratio has little effect on the aerodynamic coefficients in each direction compared to the azimuthal angle. As the aspect ratio increases from 2.0 to 2.5, the change in peak-to-peak values of C_x, C_{my}, and C_{mz} is −4.8%, 1.5%, and −10.9%, respectively, and the maximum change is −5.1%, 32.0%, and −11.8%, respectively. The peak-to-peak values of the drag coefficient and the pitching moment coefficient decrease, whereas the peak-to-peak and maximum values of the azimuthal moment coefficient increase. In addition, when $\mathrm{AR} > 2$, the aerodynamic coefficients are less sensitive to a change in the aspect ratio. Note that as the antenna aspect ratio increases from 0.5 to 2.5, the lag of the corresponding azimuthal angle when the C_{my} peak appears exceeds 65°.

3.3. Mean, Maximum, and Root Mean Square Values of Aerodynamic Coefficients with Respect to the Aspect Ratio. The selection of driving motor power of a radar antenna and the calculation of transmission structure strength should consider the aerodynamic characteristics of the antenna. In general, the root mean square value of the aerodynamic coefficient is taken as the design basis, and the maximum aerodynamic coefficient is taken as the possible maximum wind load [28]. This section discusses the correlations between the antenna aspect ratio and the mean, maximum, and root mean square values of aerodynamic coefficients. We use quantitative data to describe and analyze the influence of the antenna aspect ratio on aerodynamic characteristics. Table 2 shows the change in mean, maximum, and root mean square values of aerodynamic coefficients with aspect ratio when an antenna rotates azimuthally at reduced frequencies of $K = 0.12$ and 0.2 in a single rotation period. Because the design of the antenna structure is mainly focused on the values of aerodynamic coefficients [28], the data in the table do not indicate a direction, and the values represent magnitude only. It can be seen from the table that the mean values are the smallest, and the root mean square values are between the mean values and the maximum values. Among the mean, maximum, and root mean square values of the aerodynamic coefficients in all directions, the azimuthal moment coefficient is the smallest, and the mean, maximum, and root mean square values of the drag coefficient and the pitching moment coefficient are relatively larger.

Figure 7 shows the change in mean, maximum, and root mean square values of the aerodynamic coefficients with respect to the aspect ratio when the reduced frequency $K = 0.12$ and $K = 0.2$. When the antenna aspect ratio increases, the mean, maximum, and root mean square values of C_{mx}, C_{my}, and C_{mz} all decrease to varying degrees; the maximum and root mean square values decrease greatly. An experimental study on the aerodynamic characteristics of an antenna [22] showed that the larger the rotation radius of the antenna, the smaller the peak value and root mean square

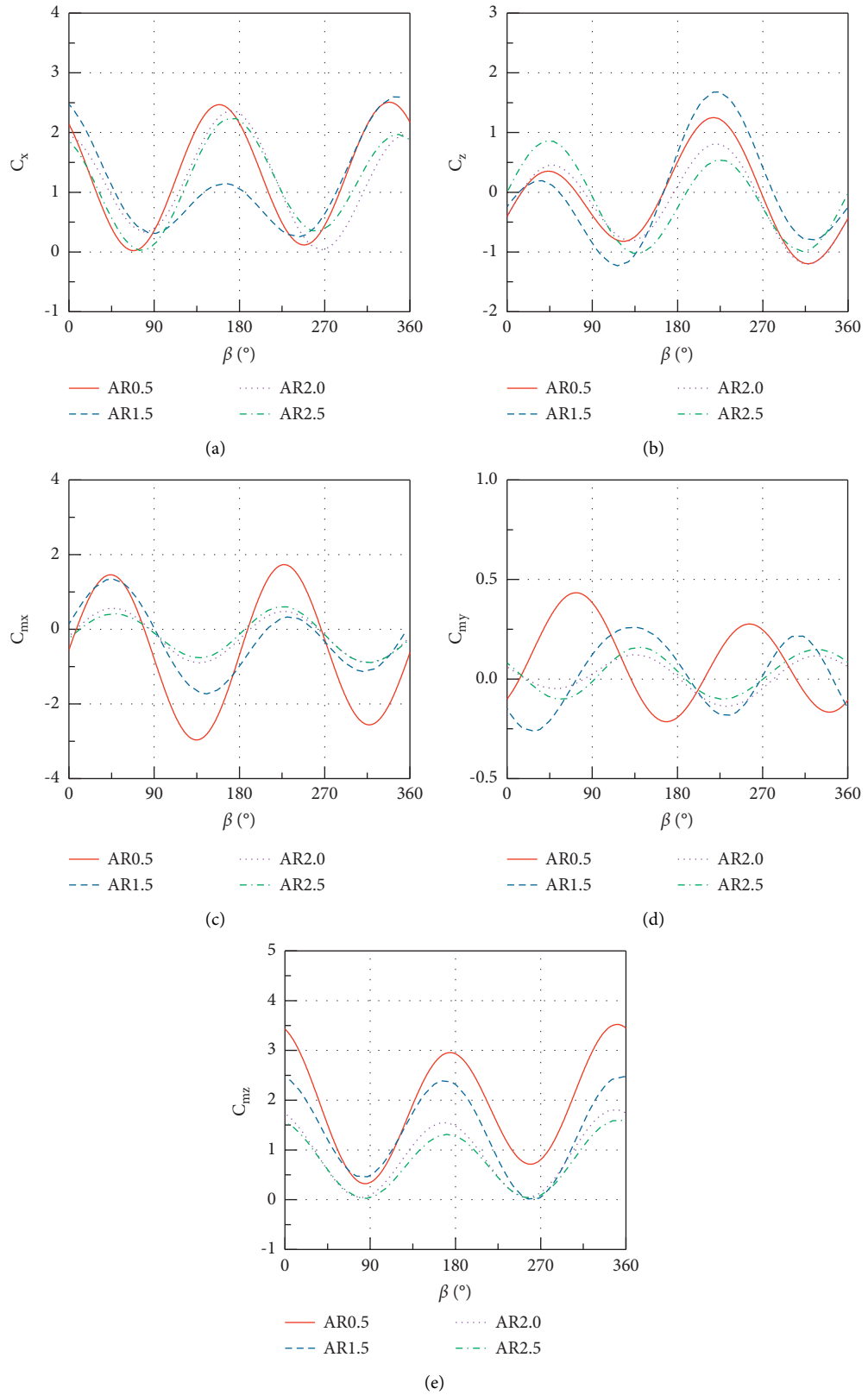

Figure 6: Aerodynamic coefficients with respect to the aspect ratio: (a) $C_x - \beta$, (b) $C_z - \beta$, (c) $C_{mx} - \beta$, (d) $C_{my} - \beta$, and (e) $C_{mz} - \beta$ ($K = 0.2$).

Table 2: Mean, maximum, and root mean square values of aerodynamic coefficients with respect to the aspect ratio during a single rotation period. AR, aspect ratio. (Values represent magnitude only, not direction).

Flat plate antenna		Reduced frequency, $K = 0.12$			Reduced frequency, $K = 0.2$		
		Mean	Maximum	Root mean square	Mean	Maximum	Root mean square
AR 0.5	C_x	0.90	1.77	1.07	1.28	2.51	1.54
	C_z	0.29	1.18	0.68	0.09	1.25	0.72
	C_{mx}	0.30	1.89	1.04	0.58	2.96	1.66
	C_{my}	0.02	0.22	0.11	0.09	0.43	0.22
	C_{mz}	1.56	2.89	1.77	1.88	3.52	2.12
AR 1.5	C_x	1.11	2.14	1.32	1.12	2.37	1.38
	C_z	0.11	0.57	0.33	0.01	1.69	0.86
	C_{mx}	0.27	1.32	0.79	0.29	1.73	0.94
	C_{my}	0.00	0.15	0.08	0.02	0.26	0.17
	C_{mz}	1.05	2.20	1.24	1.33	2.48	1.55
AR 2.0	C_x	1.08	1.99	1.23	1.15	2.25	1.34
	C_z	0.16	0.96	0.61	0.15	0.96	0.61
	C_{mx}	0.19	1.03	0.57	0.19	0.90	0.54
	C_{my}	0.04	0.19	0.11	0.01	0.14	0.08
	C_{mz}	0.82	1.74	0.99	0.86	1.81	1.04
AR 2.5	C_x	1.02	2.23	1.21	1.15	2.25	1.34
	C_z	0.10	1.04	0.57	0.10	1.04	0.57
	C_{mx}	0.13	0.91	0.50	0.16	0.90	0.51
	C_{my}	0.04	0.20	0.12	0.03	0.16	0.09
	C_{mz}	0.69	1.42	0.82	0.74	1.60	0.90

value of the azimuthal moment coefficient. A similar conclusion can be gleaned from Figure 7(d). It is worth noting that when the reduced frequency $K = 0.12$, the mean, maximum, and root mean square values of the azimuthal moment coefficient exhibit a monotonically decreasing change with respect to an increase in the aspect ratio; when the reduced frequency $K = 0.2$, they decrease with respect to an increase in the aspect ratio. As the antenna rotates, the azimuthal moment coefficient increases with respect to the aspect ratio, and it does not show a monotonic decrease. The azimuthal moment is related to the antenna aspect ratio and the reduced frequency. In the antenna design stage, the peak value of the azimuthal moment can be reduced by increasing the antenna aspect ratio; when the antenna is working, the peak value of the azimuthal moment can be reduced by reducing the reduced frequency. The mean, maximum, and root mean square values of C_x and C_z do not show obvious monotonicity with an increase in the aspect ratio. Compared to the mean values, the maximum and root mean square values of the aerodynamic coefficients are more sensitive to a change in the aspect ratio.

The aspect ratio is a key parameter affecting the aerodynamic characteristics of the antenna. Under the same reduced frequency, increasing the antenna aspect ratio can significantly reduce the average, maximum, and root mean square values of the rolling moment coefficient, the azimuthal moment coefficient, and the pitching moment coefficient. Moreover, a higher aspect ratio can suppress the sensitivity of the mean, maximum, and root mean square values of the aerodynamic coefficients to a change in the reduced frequency.

It can be seen from Figure 6(b) that the lateral force coefficients of the antennas with different aspect ratios in azimuth rotation all show the maximum value near the azimuth angle $\beta = 220^{\circ}$. Although the reduced frequencies of antennas with different aspect ratios are the same, their wind speeds are different, resulting in the maximum value of the lateral force coefficient of the antenna when $K = 0.2$ and AR = 1.5. In order to analyze the cause of this phenomenon, Figure 8 shows the vorticity nephogram of the ZOX plane when $\beta = 220^{\circ}$ and $K = 0.2$ for antennas with different aspect ratios, in which the red area indicates that the vorticity distribution in this area is dense and the blue area indicates that the vorticity distribution in this area is sparse. As shown in the figure, when AR = 0.5, the shedding vortex generated by the incoming flow passing through the support rod covers one side of the antenna array and is located at serial number one. When AR = 1.5, the shedding vortex generated by the support rod does not cover one side of the antenna array, and more shedding vortices are generated at the edge of the other side of the antenna compared with AR = 0.5, 2.0, and 2.5, as shown in serial number three. When AR = 2.0 or 2.5, the shedding vortices on both sides of the antenna are significantly weakened. Because the center of the vortex core is negative pressure, the pressure in the area with dense vorticity is lower so that the antenna receives large suction in the positive direction of the Z-axis, which explains the reason for the maximum value of the lateral force coefficient when $K = 0.2$ and AR = 1.5.

In order to analyze the shedding characteristics of the vortex during antenna azimuth rotation, the vorticity at the two monitoring points is monitored during numerical simulation, as shown in Figure 9. The variation curve of vorticity at the monitoring point relative to azimuth in a rotation cycle of the antenna is drawn. Figure 10 shows the variation curve of vorticity with antenna azimuth in a rotation cycle of radar antenna with AR = 2.5 and the results of vorticity variation processed by fast Fourier transform. It can

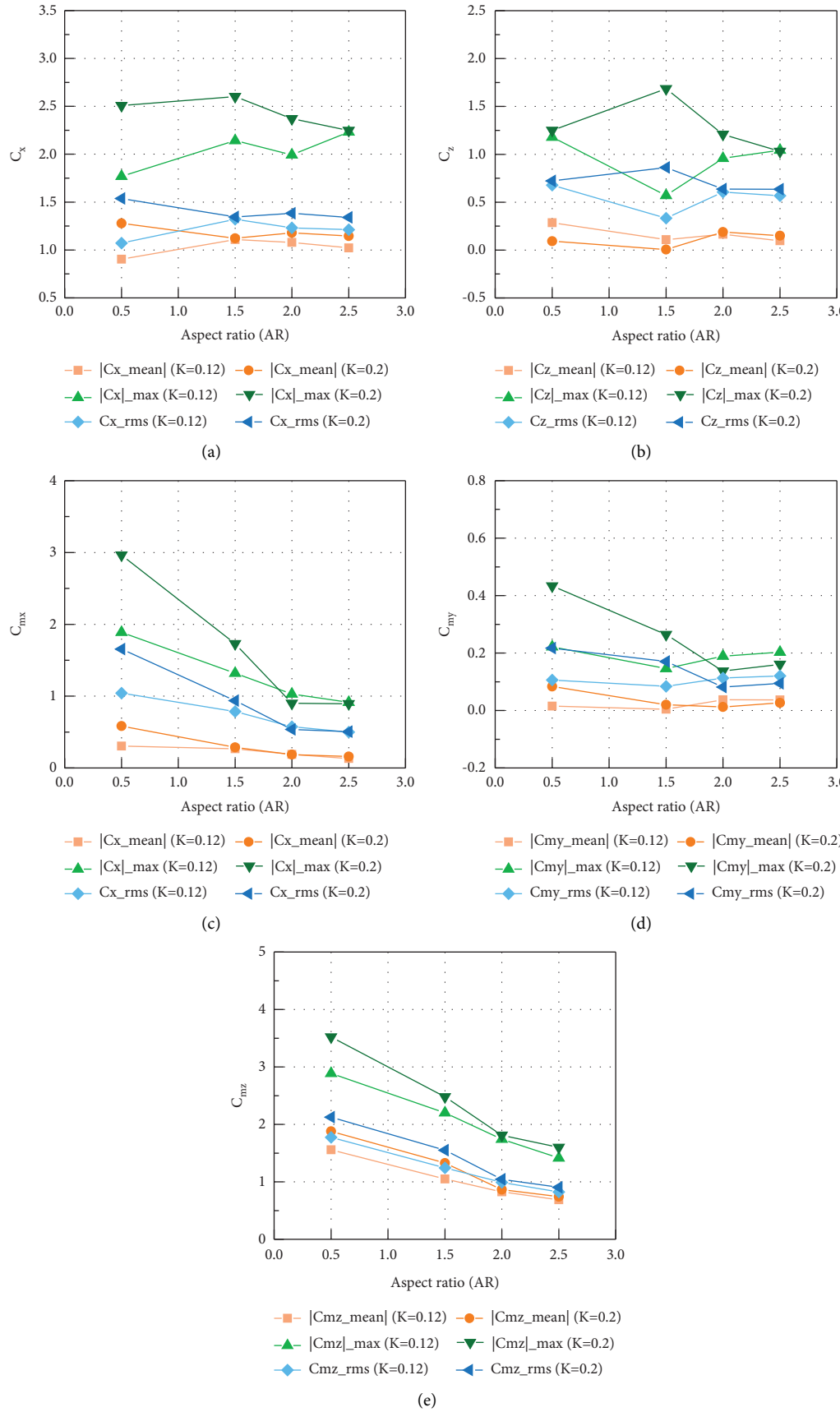

Figure 7: Mean, maximum, and root mean square values of the aerodynamic coefficients with respect to the aspect ratio when the antenna is rotating azimuthally at different reduced frequencies: (a) $C_x - \beta$, (b) $C_z - \beta$, (c) $C_{mx} - \beta$, (d) $C_{my} - \beta$, and (e) $C_{mz} - \beta$ ($K = 0.12$ and $K = 0.2$).

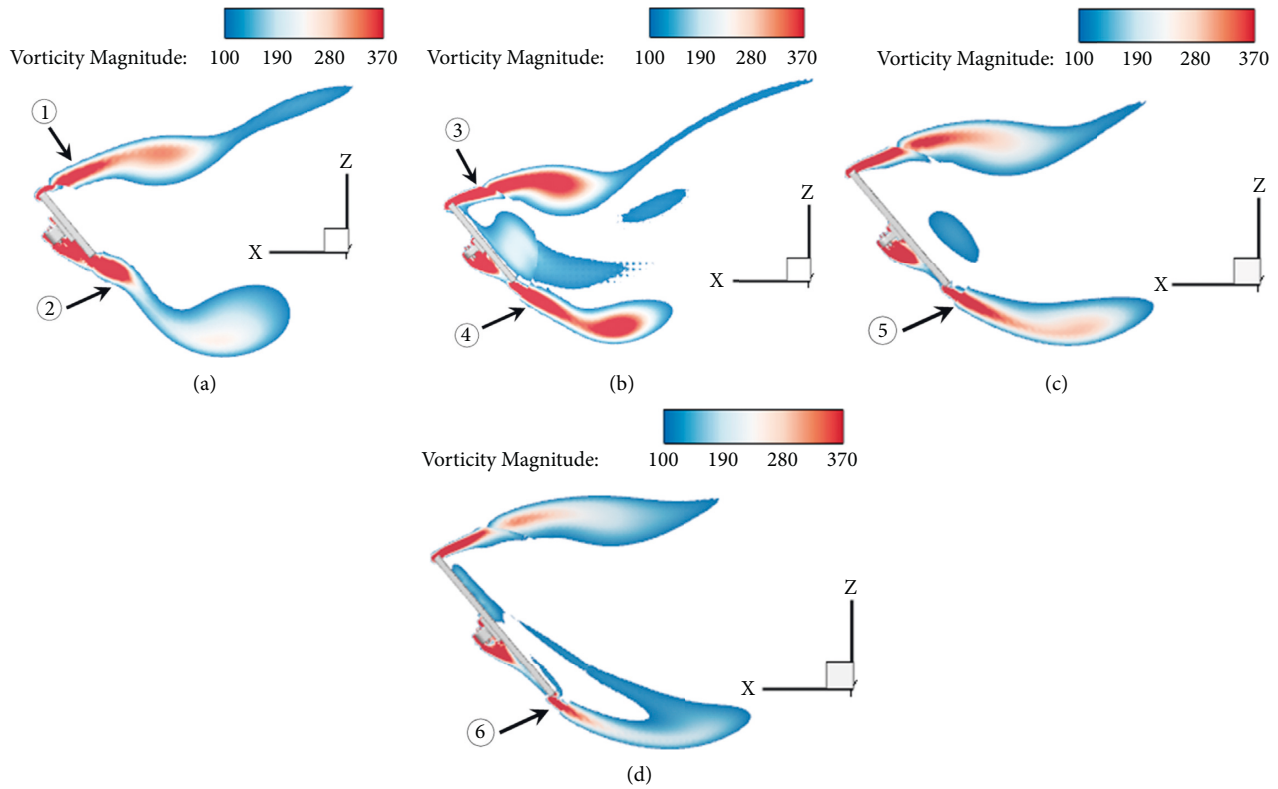

Figure 8: Variation of cloud pattern of antenna vorticity field relative to aspect ratio: (a) AR = 0.5, (b) AR = 1.5, (c) AR = 2.0, and (d) AR = 2.5 ($\beta = 220^{\circ}$, $K = 0.2$, ZOX plane, and $Y = 0$).

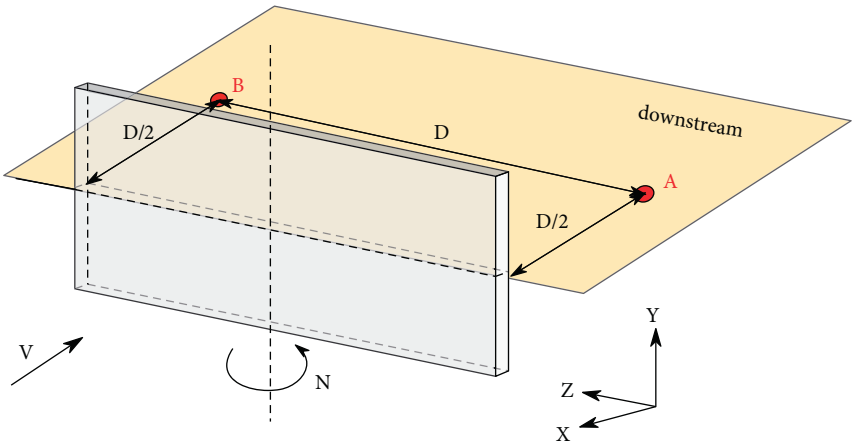

Figure 9: Schematic diagram of the location of the vorticity monitoring point downstream of the antenna (ZOX plane and $Y = 0$).

be seen from Figure 10(a) that there are two obvious positive peaks in the change of vorticity at the monitoring point in a rotation cycle, which indicates that in a rotation cycle, the antenna rotation produces two shedding vortices and passes through the monitoring point. This conclusion can also be obtained from Figure 10(b).

3.4. Mean, Maximum, and Root Mean Square Values of Aerodynamic Coefficients with Respect to the Reduced Frequency. Because the reduced frequency ranges of antennas with different aspect ratios are not the same, in this section, we discuss the change in the aerodynamic coefficients of antennas with different aspect ratios relative to their respective reduced frequency ranges. Figure 11 shows compare curves for the mean, maximum, and root mean square aerodynamic coefficients of antennas with different aspect ratios relative to the reduced frequency. When AR = 0.5 and 1.5, the mean, maximum, and root mean square values of the aerodynamic coefficients change greatly with an increase in the reduced frequency; when AR = 2.0 and 2.5, the mean, maximum, and root mean square values

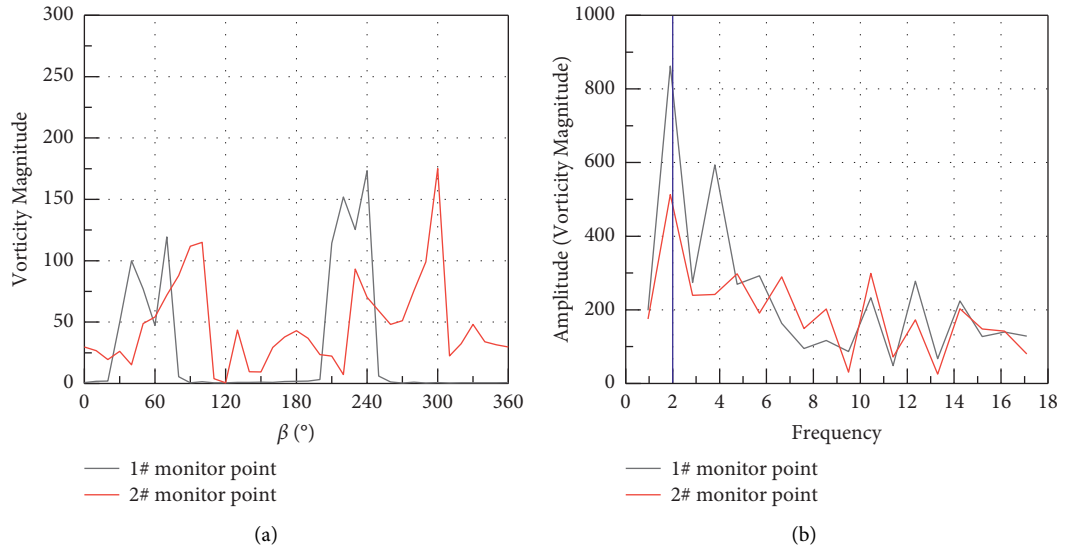

FIGURE 10: The vorticity distribution around the antenna changes with respect to the azimuth angle (AR = 2.5 and $K = 0.2$): (a) vorticity magnitude and (b) fast Fourier transform.

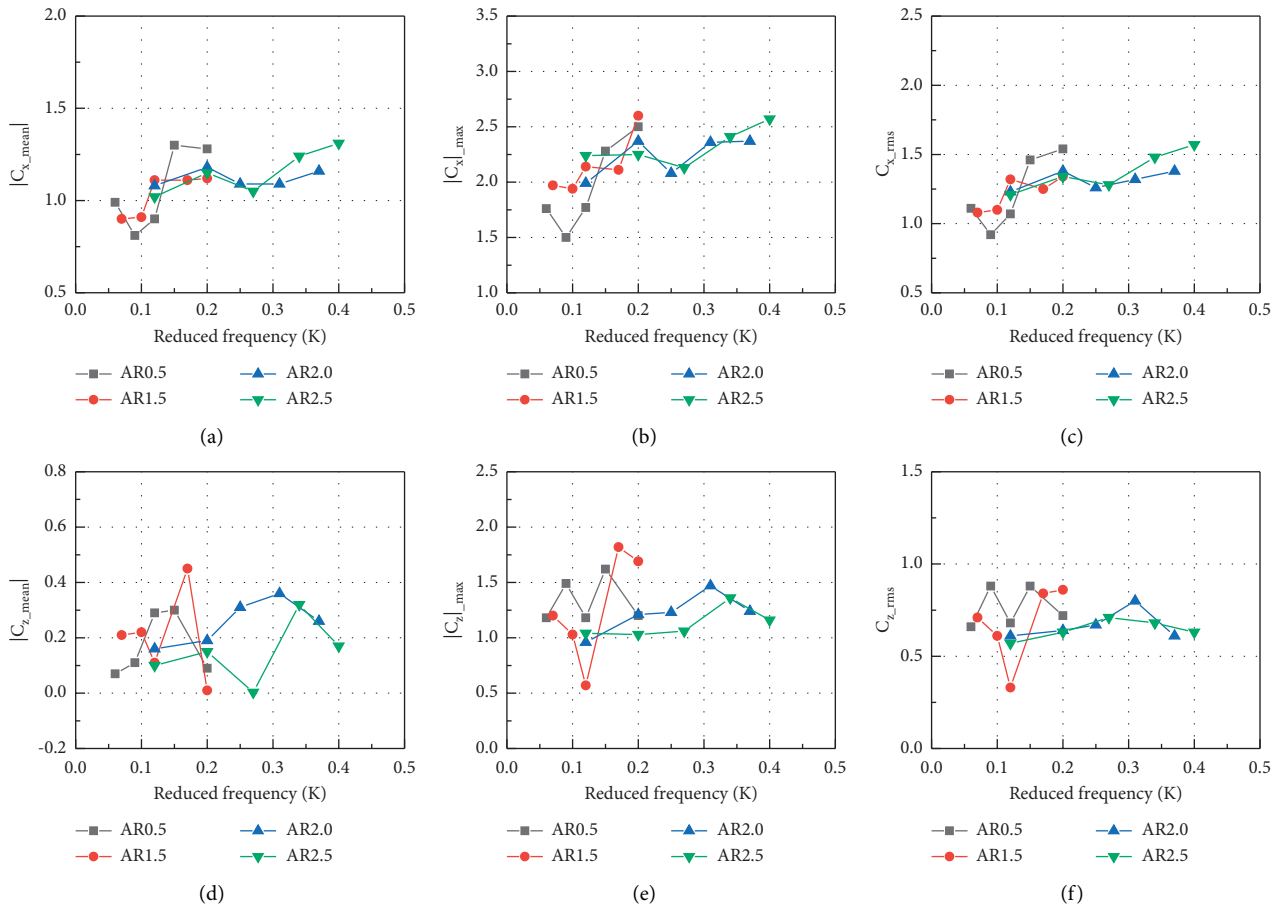

FIGURE 11: Continued.

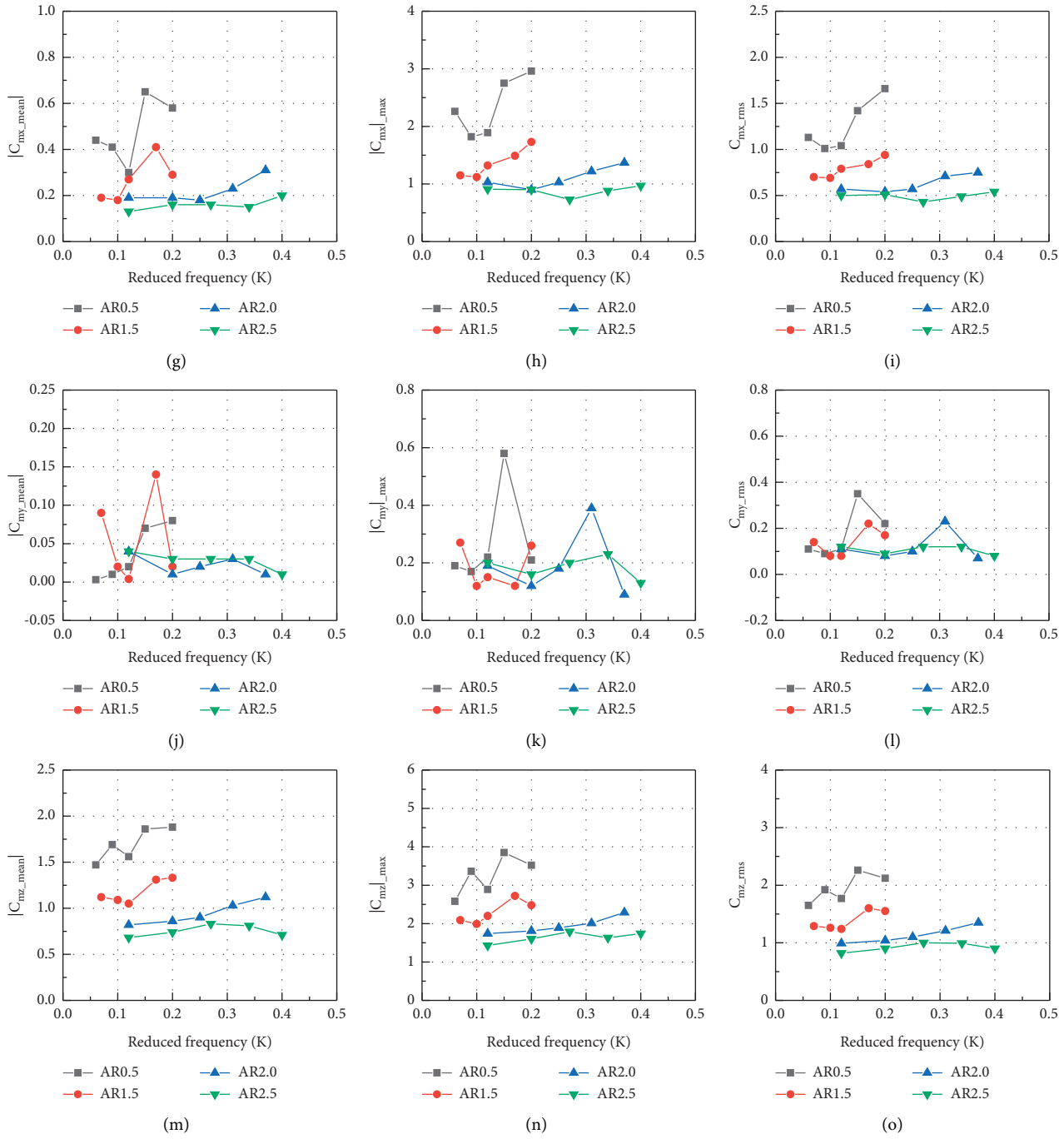

FIGURE 11: Mean, maximum, and root mean square values of the aerodynamic coefficients with respect to the reduced frequency when an antenna with different aspect ratios is rotating azimuthally: (a) $|C_{x\_mean}|$, (b) $|C_x|_{max}$, (c) C_{x_rms}, (d) $|C_{z\_mean}|$, (e) $|C_z|_{max}$, (f) C_{z_rms}, (g) $|C_{mx\_mean}|$, (h) $|C_{mx}|_{max}$, (i) C_{mx_rms}, (j) $|C_{my\_mean}|$, (k) $|C_{my}|_{max}$, (l) C_{my_rms}, (m) $|C_{mz\_mean}|$, (n) $|C_{mz}|_{max}$, and (o) C_{mz_rms}.

of C_x, C_{mx}, and C_{mz} change approximately linearly relative to the reduced frequency. Therefore, the mean, maximum, and root mean square values of the aerodynamic coefficients of a flat plate antenna with a small aspect ratio are more sensitive to a change in the reduced frequency.

With the increases of reduced frequency, when AR = 0.5, the mean change range of $|C_{x\_mean}|$, $|C_{z\_mean}|$, $|C_{mx\_mean}|$, $|C_{my\_mean}|$, and $|C_{mz\_mean}|$ exceeds 60%, 329%, 117%, 2,567%, and 28%, respectively; when AR = 1.5, the mean change range exceeds 24%, 4,400%, 128%, 3,400, and 27%, respectively; when AR = 2.0, it exceeds 9%, 125%, 72%, 300%, and 37%, respectively; and when AR = 2.5, it exceeds 28%, 10,567%, 54%, 300%, and 22%, respectively. According to Figures 11(a), 11(d), 11(g), 11(j), and 11(m), when AR = 2.0 and 2.5, the mean aerodynamic coefficients of the antenna change smoothly with respect to the reduced frequency.

When the antenna aspect ratio increases, the sensitivity of the mean aerodynamic coefficients to the reduced frequency decreases. Besides, the mean value of the aerodynamic coefficient is much smaller than the maximum value and the root mean square value.

The influence of the change in the reduced frequency on the maximum aerodynamic coefficients of antennas with different aspect ratios is analyzed below. With the increases of reduced frequency, when AR = 0.5, the maximum change range of $|C_x|_{\max}$, $|C_z|_{\max}$, $|C_{mx}|_{\max}$, $|C_{my}|_{\max}$, and $|C_{mz}|_{\max}$ exceeds 67%, 37%, 63%, 241%, and 49%, respectively; when AR = 1.5, the maximum change range exceeds 34%, 219%, 54%, 125%, and 37%, respectively; when AR = 2.0, it exceeds 19%, 53%, 52%, 333%, and 32%, respectively; and when AR = 2.5, it exceeds 21%, 32%, 33%, 77%, and 25%, respectively. According to Figures 11(b), 11(e), 11(h), 11(k), and 11(n), when AR = 2.0 and 2.5, the maximum aerodynamic coefficients of the antenna change smoothly with respect to the reduced frequency. When the antenna aspect ratio increases, the sensitivity of the maximum aerodynamic coefficients to the reduced frequency decreases. In addition, except for $|C_{mx}|_{\max}$ and $C_{my}|_{\max}$, increasing the antenna aspect ratio does not significantly reduce the maximum aerodynamic coefficient in other directions.

With the increases of reduced frequency, when AR = 0.5, the maximum change range of C_{x_rms}, C_{z_rms}, C_{mx_rms}, C_{my_rms}, and C_{mz_rms} is about 67%, 33%, 64%, 289%, and 37%, respectively; when AR = 1.5, the maximum change range is about 24%, 161%, 36%, 175%, and 29%, respectively; when AR = 2.0, it is about 12%, 31%, 39%, 229%, and 36%, respectively; and when AR = 2.5, it is about 30%, 25%, 26%, 50%, and 22%, respectively. From Figures 11(c), 11(f), 11(i), 11(l), and 11(o), we can see that when AR = 2.0 and 2.5, the root mean square values of the aerodynamic coefficients change smoothly with respect to the reduced frequency. That is, when the antenna aspect ratio increases, the sensitivity of the root mean square values of the aerodynamic coefficients to the reduced frequency decreases; in addition, except for C_{x_rms}, increasing the antenna aspect ratio can significantly reduce the root mean square value of the aerodynamic coefficient in other directions.

4. Conclusions

Through the dynamic force measurement test in the wind tunnel, the aerodynamic characteristics of rotating antennas with different aspect ratios are studied for the first time. Change in the aerodynamic coefficients of the antenna with respect to the aspect ratio and reduced frequency was determined, and the flow field structure around the antenna during rotation was analyzed by numerical simulation. The following conclusions are drawn.

When antennas with different aspect ratios rotate azimuthally, the aerodynamic coefficients show cyclical change similar to a sine curve with respect to the azimuthal angle. The results of the aerodynamic coefficient tests show that the aspect ratio is the key design parameter affecting the aerodynamic characteristics of the antenna.

The experimental results indicate that the magnitude of the azimuthal moment is related to the antenna aspect ratio and the reduced frequency. The antenna aspect ratio and reduced frequency significantly impact the mean, maximum, and root mean square values of aerodynamic coefficients. With the increase of reduced frequency, when AR = 0.5, the maximum change range of $|C_x|_{\max}$, $|C_z|_{\max}$, $|C_{mx}|_{\max}$, $|C_{my}|_{\max}$, and $|C_{mz}|_{\max}$ exceeds 67%, 37%, 63%, 241%, and 49%, respectively; when AR = 1.5, the maximum change range exceeds 34%, 219%, 54%, 125%, and 37%, respectively; when AR = 2.0, it exceeds 19%, 53%, 52%, 333%, and 32%, respectively; and when AR = 2.5, it exceeds 21%, 32%, 33%, 77%, and 25%, respectively. In the antenna design stage, the peak value of the azimuthal moment can be reduced by increasing the antenna aspect ratio; when the antenna is working, the peak azimuthal moment can be reduced by reducing the reduced frequency.

Data Availability

The data that support the findings of this study are available from the corresponding author upon reasonable request.

Conflicts of Interest

The authors declare that there are no conflicts of interest regarding the publication of this paper.

Acknowledgments

This work was supported by the Priority Academic Program Development of Jiangsu Higher Education Institutions (PAPD).

References

[1] A. A. Althuwayb and D. Chaturvedi, "Substrate Integrated Waveguide Based Cavity-Backed Bowtie-Slot antenna-triplexer," *International Journal of RF and Microwave Computer-Aided Engineering*, 2021.

[2] A. Kumar and M. Hasan, "A coplanar-waveguide-fed planar integrated cavity backed slotted antenna array using TE33 mode," *International Journal of RF and Microwave Computer-Aided Engineering*, vol. 30, no. 10, 2020.

[3] A. Kumar, A. A. Althuwayb, and J. Al-Hasan, "Wideband triple resonance patch antenna for 5G wi-fi spectrum," *Progress In Electromagnetics Research Letters*, vol. 93, 2020.

[4] Z. Li and Z. Wang, "Research on the wind-resistant stability of large vehicle-borne radar," *Electro-Mechanical Engineering*, vol. 31, no. 3, pp. 11–15, 2015.

[5] R. B. Blaylock, B. Dayman, and N. L. Fox, "Wind tunnel testing of antenna models," *Annals of the New York Academy of Sciences*, vol. 116, no. 1, pp. 239–274, 1964.

[6] J. D. Holmes, *Wind Loading of structures*, CRC Press, London, UK, 2015.

[7] J. Y. R. Bicknell, "Air Loads and Pressure Distribution on a Parabolic antenna model," 1962.

[8] F. Bian and W. Sun, "Research on anti-overturning fatigue of a microwave intelligence radar under wind load," *Electro-Mechanical Engineering*, vol. 36, no. 3, pp. 26–29, 2020.

[9] H. Schippers, H. van Tongeren, J. Verpoorte, and G. Vos, "Distortion of Conformal antennas on aircraft Structures,

2001," *SPIE, Proceedings of the Smart Electronics and MEMS,SPIEi*, vol. 4334, 2001.

[10] W. Gawronski, J. A. Mellstrom, and B. Bienkiewicz, "Antenna mean wind torques: a comparison of field and wind-tunnel data," *IEEE Antennas and Propagation Magazine*, vol. 47, no. 5, pp. 55–59, 2005.

[11] B. Gumusel, C. Camci, and C. Camci, "Aerodynamic drag characteristics and shape design of a radar antenna used for airport ground traffic control," *Progress in Computational Fluid Dynamics, An International Journal*, vol. 10, no. 1, pp. 32–39, 2010.

[12] L. N. Fox, *Experimental Data on Wind-Induced Vibrations of a Paraboloidal Reflector antenna model*, Jet Propulsion Laboratory and California Institute of Technology, Pasadena, CA, USA, 1963.

[13] W. K. Gawronski and J. A. Mellstrom, *Field Verification of the Wind Tunnel coefficients*, Jet Propulsion Laboratory and California Institute of Technology, Pasadena, CA, USA, 1994.

[14] P. Sachs, *Wind Forces in engineering*, Pergamon Press, Oxford, UK, 1978.

[15] S. Muggiasca, F. Ripamonti, D. Rocchi, and A. Zasso, "Numerical and experimental investigation on a maritime radar scanner," in *Proceedings of the Fluid Structure Interaction*, Crete, Greece, 2009.

[16] A. Scarabino, M. G. Sainz, F. Bacchi, J. S. Delnero, and A. Canchero, "Numerical and experimental study of unsteady wind loads on panels of a radar aerial," *Wind and Structures*, vol. 23, no. 1, pp. 1–18, 2016.

[17] C. Camci and B. Gumusel, "Vortex shedding from a ground tracking radar antenna and 3D tip flow characteristics," *Progress in Computational Fluid Dynamics, An International Journal*, vol. 13, no. 5, pp. 263–269, 2013.

[18] G. Lombardi, "Wind-tunnel tests on a model antenna rotating in a cross flow," *Engineering Structures*, vol. 13, no. 4, pp. 345–350, 1991.

[19] C. Goyal, A. S. Poyyamozhi, S. John, and T. Chauhan, "Antenna system structural and aerodynamic analyside application of airborne," *Materials Today Proceedings*, 2020.

[20] R. Weerasinghe and T. Bunn, "Wind load assessment of a large radar antenna using measurements and simulation," *IOP Conference Series: Earth and Environmental Science*, vol. 94, pp. 012194–12216, 2017.

[21] S. Qiao and J. Gu, "Effect and evaluation of wind-load to radar pedestal," *Modern Radar*, vol. 39, no. 10, pp. 95–99, 2017.

[22] W. Xiao, "Wind load factor of an antenna with double curvature reflector," *Electro-Mechanical Engineering*, no. 6, pp. 55–61, 1996.

[23] F. Gustafsson, "Determining the initial states in forward-backward filtering," *IEEE Transactions on Signal Processing*, vol. 44, no. 4, pp. 988–992, 1996.

[24] Y. Zhang and Z. Zhang, "Unsteady aerodynamic characteristics of antenna rotating in different elevation angles," *International Journal of Antennas and Propagation*, vol. 2021, Article ID 5503330, 16 pages, 2021.

[25] Y. Zhang and Z. Zhang, "Aerodynamic characteristics of radar antenna in stationary and azimuthal rotational motion," *International Journal of Antennas and Propagation*, vol. 2021, Article ID 6950615, 23 pages, 2021.

[26] D. M. Hargreaves, B. Kakimpa, and J. S. Owen, "The computational fluid dynamics modelling of the autorotation of square, flat plates," *Journal of Fluids and Structures*, vol. 46, pp. 111–133, 2014.

[27] X. Ortiz, D. Rival, and D. Wood, "Forces and moments on flat plates of small aspect ratio with application to PV wind loads and small wind turbine blades," *Energies*, vol. 8, no. 4, pp. 2438–2453, 2015.

[28] L. Ping, P. Huang, and R. Zhang, *Radar Structure and technology*, Electronic Industry Press, China, Beijing, 2007.